

Vibrational spectra and normal coordinate analysis of crystalline H_2O_2 , D_2O_2 and HDO_2

JOSE L. ARNAU and PAUL A. GIGUÈRE

Centre de Recherches sur les Atomes et les Molécules, Université Laval,
Québec, Canada

and

MOTOKO ABE and ROBERT C. TAYLOR

Department of Chemistry, The University of Michigan, Ann Arbor,
Michigan, U.S.A.

(Received 11 April, 1973)

Abstract—A systematic investigation has been carried out of the vibrational spectra of the hydrogen peroxide crystal and its deuterated analogue, using both i.r. and Raman spectroscopy, over the range $4000\text{--}50\text{ cm}^{-1}$. Mixtures of the two isotopic species up to approximately 95% deuteration were also studied to identify the fundamentals of the hybrid molecule, HDO_2 . Single crystals of hydrogen peroxide oriented along two of the three crystallographic axes were examined in the Raman effect with polarized laser light. The O—H stretching bands are remarkably narrow in the Raman spectra: $\Delta\nu(\frac{1}{2}) = 20\text{ cm}^{-1}$ at -193°C compared with about 80 cm^{-1} in the i.r. Nearly all the O—H stretching components predicted by the factor group analysis were observed but a satisfactory identification of all components of the OOH deformation modes could not be achieved. The O—O stretching frequency in D_2O_2 (872 cm^{-1}) is slightly higher than in H_2O_2 (871 cm^{-1}) contrary to expectations. The hydrogen bonds in the H_2O_2 crystal appear somewhat less strong (by about 10–15%) than those in ice.

A normal coordinate analysis of the unit cell modes proved to be of considerable value in the assignment of observed frequencies. The values of the eleven principal force constants and the twenty interaction constants used to fit the 59 assigned frequencies appear reasonable and are comparable with values found for other hydrogen bonded systems.

INTRODUCTION

THE HYDROGEN peroxide molecule has always been of special interest since it is the simplest molecule featuring internal rotation about a single bond. The dynamics of the H_2O_2 crystal equally deserve attention in connection with the closely related and important problem of ice. A number of structural and spectroscopic investigations have been reported since the early Raman and i.r. work of the authors [1, 2]. Despite these various investigations, several unanswered questions remain. In particular, observation and assignments of the OH bending modes are still in an unsatisfactory state and no clear distinction has been made between bands arising from the internal rotation mode of the molecules and one of the external librational motions of the molecules in the crystal lattice. Many of the existing data have been taken at different temperatures and correlation of the results of different workers is difficult due to a significant but undetermined temperature effect on frequencies.

In the present work, the existing data have been extended to include both i.r. and Raman results on the isotopic species D_2O_2 . In addition, polarization results

[1] R. C. TAYLOR, *J. Chem. Phys.* **18**, 898 (1950).

[2] O. BAIN and P. A. GIGUÈRE, *Can. J. Chem.* **33**, 527 (1955).

from the Raman spectra of single crystal hydrogen peroxide [3] have been extended using laser excitation. The isotope dilution technique was applied in an attempt to identify the various crystal field effects and to ascertain the fundamental vibrations of the mixed HDO_2 species. All available data were then used in carrying out a normal coordinate analysis of the spectrum of the crystal. This work was nearly completed when a recent paper by LANNON *et al.* [4] came to our attention. Their data on the i.r. spectra of H_2O_2 and D_2O_2 in the region of the fundamentals are essentially the same as ours, but there are some differences in interpretation.

EXPERIMENTAL

Pure anhydrous hydrogen peroxide was prepared by fractional distillation under reduced pressure of a 90% commercial solution (Buffalo Electro-Chemical Co.). The residual water content, some 0.5%, was removed in the mother liquor from a large single crystal as described previously [5]. Deuterium peroxide was produced by the electrical discharge method [6] from heavy water of 99.5% D content. Repeated fractional distillation raised the peroxide concentration from about 60 to 98–99 per cent. Because of the very rapid isotopic exchange [7] with water absorbed on the walls of the glass vessels it was not possible to retain the initial high isotopic purity. The average hydrogen contamination in the final sample was of the order of 5 per cent, judging from the intensity of the residual OH bands at $3\ \mu$ in the i.r. These bands, which at times have erroneously been assigned to combination modes of the D_2O_2 molecule, are also present in the recently published i.r. spectra of the crystalline peroxides [4]. This small isotopic contamination does not significantly alter the spectrum of the major component judged by the reciprocal case of H_2O_2 slightly contaminated by D_2O_2 .

For the i.r. studies, the samples were prepared by condensation of the vapor on a disc of Irtran-6 (Eastman Kodak Co.) cooled to liquid nitrogen temperatures in an evacuated glass cell fitted with CsBr windows. Alkali halides cannot be used to support the peroxide films because of a tendency to react slowly at temperatures above -120° , presumably forming peroxyhydrates analogous to the addition compound, $\text{KF}\cdot\text{H}_2\text{O}_2$ [8]. The fundamental frequencies of hydrogen peroxide deposited on alkali halide supports are quite different from those of the pure crystal [4]. Deposition of hydrogen peroxide from the vapor on a substrate at liquid nitrogen temperatures invariably produces a vitreous phase and the film must be warmed to initiate crystallization. This was observed to begin at about -120° with the appearance of tiny rosette-shaped centers that grew slowly upon gradual warming up to about -80° at which point they covered the whole window with a powdery appearing film. For a homogeneous sample the temperature had to be uniform

-
- [3] R. C. TAYLOR, Symposium on Molecular Structure and Spectroscopy. Columbus, Ohio, in *Spectrochim. Acta* **10**, 222 (1957).
[4] J. A. LANNON, F. D. VERDERAME and R. W. ANDERSON, JR., *J. Chem. Phys.* **54**, 2212 (1971).
[5] P. A. GIGUÈRE, *Bull. Soc. Chim. France* 720 (1954).
[6] P. A. GIGUÈRE, E. A. SECCO and R. S. EATON, *Discuss. Faraday Soc.* **14**, 104 (1953).
[7] M. ANBAR, A. LOEWENSTEIN and S. MEIBOOM, *J. Am. Chem. Soc.* **80**, 2630 (1958).
[8] P. A. GIGUÈRE and HÉLÈNE ROY, *Rev. Chim. Min.* **7**, 1053 (1970).

across the entire window. Otherwise some phase segregation remained, as revealed by the spectra.

One point which must be stressed here is the difficulty of getting absolutely pure hydrogen peroxide samples for i.r. study. Although an essentially anhydrous (approaching 99.97%) [5] product can be prepared by repeated fractional crystallization, the technique of deposition from the vapor invariably introduces some slight catalytic decomposition on the walls of the vacuum system and absorption cell. Since water is more volatile than hydrogen peroxide, it condenses preferentially on the cold window. Upon crystallization of the vitreous film traces of the dihydrate are formed which have their own characteristic frequencies [9, 10].

In contrast to the i.r. case, samples for Raman studies can be prepared as essentially anhydrous material in the form of single crystals. The early data discussed in Ref. [3] were obtained from large single crystals approximately 10 mm in dia. and 10–12 cm long. These were grown by the Stockbarger method in which a Pyrex cell containing 99.8%+ peroxide was lowered through a sharp temperature gradient at a rate of about 2 mm per hour. The apparatus was maintained in a cold room at a constant temperature of -10° . Crystallization was induced by touching the tip of the capillary at the end of the cell with dry ice or liquid nitrogen. Since the preferential growth direction of the crystal is along the z-axis of the tetragonal unit cell, the single crystal which eventually resulted usually was oriented with its z-axis parallel to the axis of the tube. When about 80 per cent of the material had crystallized, the supernatant liquid was removed with a pipette leaving a perfectly flat and clear upper surface to the crystal through which the scattered light could be observed. Before examination, the crystal was checked optically for proper orientation.

For the polarization measurements with the laser light source, the sample tube was a capillary some 3 mm in dia. with its end drawn out to a fine tip. Single crystals were grown similarly to the larger ones by lowering the cell, once crystallization had been initiated at the tip, into a liquid bath at about -5° at a rate of 3–4 mm per hr. Specimens having gas bubbles, poor orientations or other faults were discarded. These single crystals were never cooled below -30° to avoid cracking. For the Raman spectra, the single crystals were mounted coaxially inside a vacuum jacketed cell through which cooled dry nitrogen gas was circulated. In the case of the capillary sample, the single crystal could be rotated about its long axis by means of ground joint (Fig. 1).

Infrared spectra were recorded with a Perkin-Elmer Model 621 spectrometer. The Raman spectra of the larger crystals at -10° were obtained photographically using a helical Toronto Hg arc source and a Gaertner spectrograph with appropriate filtering of the exciting light. Polarization data were obtained using Polaroid cylinders. The more detailed polarization results on the smaller crystals were obtained with the 4880 Å line of an argon ion laser (Coherent Radiation Model 52), a Spex double monochromator (Model 14-II) and an ITT FW-130 photomultiplier. A quartz polarizer (Ednolite) and scrambler were used in the polarization measurements. For the stronger, sharper bands in both spectra, estimated uncertainties in

[9] P. A. GIGUÈRE and K. B. HARVEY, *J. Mol. Spectry*, **3**, 36 (1959).

[10] J. L. ARNAU and P. A. GIGUÈRE, *Can. J. Spectry*, **17**, 121 (1972).

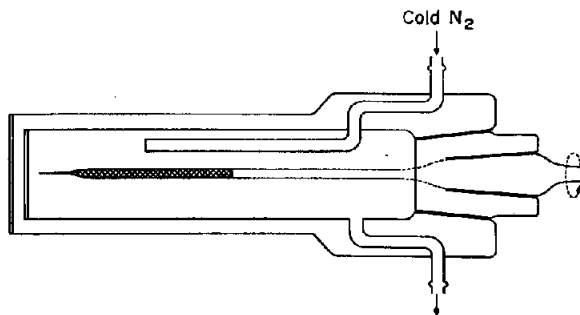


Fig. 1. Low temperature cell for the Raman spectra of oriented single crystals of H_2O_2 .

frequency are of the order of 1 cm^{-1} with somewhat higher values for the weaker and more diffuse bands.

RESULTS

The i.r. spectra of crystalline hydrogen peroxide are not reproduced here since no significant differences were found with those published previously [9]. The same is true of the far i.r. spectra of the two isotopic peroxides [11]. In the fundamental region, however, the present frequencies for D_2O_2 (Table 1) are more accurate than the previous ones. As expected, the isotopic mixtures revealed several new features of interest (Table 2, Fig. 2). The concentrations of each of the three isotopic species shown in Table 3 were estimated from the bulk composition (by weighing) of the mixtures assuming an equilibrium constant of 4 for the exchange reaction.

Raman spectra were recorded only for the H_2O_2 and D_2O_2 crystals (Figs. 3 and 4). The isotopic dilution experiments could not be expected to add much significant information because of the number of active components, especially for the OH (or OD) stretching modes. However, the isotopic contamination in the D_2O_2 sample revealed the single OH stretching band of the hybrid species at 3236 cm^{-1} , the same frequency as in the i.r. spectrum. Likewise, the Raman spectrum of a crystal containing 5% of D_2O_2 in H_2O_2 showed the OD stretching of the hybrid molecule at exactly the same frequency as in the i.r. The polarized Raman spectra of the single H_2O_2 crystal shown in Figs. 5 and 6 are identified according to the notation of DAMEN *et al.* [12]. Only the spectra corresponding to the following components of the polarizability tensor could be obtained: α_{xy} , α_{xz} , α_{yz} and α_{zz} . Unfortunately, the small crystals could not be studied by illumination along the major (Oz) axis of the crystal since this required cutting off the tip of the capillary. When this was tried, apparently the broken end of the crystal partly depolarized the laser light.

DISCUSSION OF ASSIGNMENTS

Since the crystal structure of hydrogen peroxide is known from diffraction studies [13, 14], the vibrational spectrum of the crystal can be interpreted in terms

[11] P. A. GIGUÈRE and C. CHAPADOS, *Spectrochim. Acta* **22**, 1131 (1966).

[12] T. C. DAMEN, S. P. S. PORTO and S. B. TELL, *Phys. Rev.* **142**, 570 (1966).

[13] S. C. ABRAHAMS, R. L. COOLIN and W. M. LIPSCOMB, *Acta Cryst.* **4**, 15 (1951).

[14] W. R. BUSING and H. A. LEVY, *J. Chem. Phys.* **42**, 3054 (1965).

Table 1. Principal bands in the i.r. and Raman spectra of crystalline H₂O₂ and D₂O₂ (cm⁻¹)

263°K *	H ₂ O ₂		Infrared		Raman		D ₂ O ₂		
	Raman						Infrared		
	190°K	80°K	90°K †	4°K †	190°K	80°K	90°K	90°K	
3332	3315	3304			2467	2455			$\nu_1(B_2)$
3317	3296	3285	3292	3285	~2455	2440	2439	2530	$\nu_1(E)$
	3228	3208			2405	2391			$\nu_3(B_1)$
3229	3208	3187	3182	3175	2390	2376	2375	2400	$\nu_5(E)$
3198	3178	3155			2371	2353			$\nu_1(A_1)$
							~2350		$\nu_5(A_2)$
2825	~2840	~2830	2840	2840	~2080	~2090	2090	2100	$\nu_2 + \nu_6$
2746	~2760	~2760	2745		~2042	~2045	2041	2050	$2\nu_6$
1410	1418	1421			1035	1038	1065		$\nu_3(A_1, E)$
			1410	1410			1048	1070	$\nu_6(A_2)$
1377	1383	1385	1385	1390	1021	1023	1024	1030	$\nu_2(B_2), \nu_6(E, B_1)$
			1332	1345			990	950	(656 + 690)
									(486 + 514)
880	881	881	880	880	882	882	882	880	$\nu_3(A_1, E, B_1, E)$
			809	815					(151 + 690?)
704	720	742			530	553			$\nu_4(A_1)$
			690	695			591	585	(E)
			656	661			514	511	$\nu_4(E, A_2?)$
							486	482	(A ₂)
690	619	637			456	467			$\nu_4(B_2)$
289	303	317	‡		289	302			(B ₁)
		281				264			(87 + 195)
257	267	276			250	260			(87 + 195)
245	254	264	259		238	248		244	(E)
			236					230	(A ₂)
207	215	225	219		208	216		210	(E)
182	189	195	192		179	184		188	(A ₁)
143	154	161			145	154			(B ₂)
	146	152	151			149		148	(E)
114	126	131			122	127			(A ₂)
			109					105	(A ₁)
78	84	87			82	84			(B ₂)

* Ref. [3].

† Ref. [9].

‡ Ref. [11].

of group theory under the factor group approximation. In the construction of the correlation diagram, some confusion arises over the question of whether the molecular C₂-axis should be identified with the C₂' or the C₂"-axis of the D₄ unit cell group. Character tables in most standard references [15] are of no direct help in this question since the orientations of the C₂-axes with respect to the coordinate frame of reference are not specified (see, however, Ref. [16]). The ambiguity can be resolved by examining the transformation properties of the polarizability components. When this is done, it is found that the molecular C₂-axis must be identified with the diagonal C₂"-axis of the unit cell group leading to the correlation diagram shown in Fig. 7. This diagram differs from that used by MILLER and HORNING [17] and

[15] E. B. WILSON, JR., P. C. CROSS and J. C. DECUS, *Molecular Vibrations*, McGraw-Hill, New York (1955).

[16] L. L. BOYLE, *Acta Cryst.* **A27**, 76 (1971).

[17] R. L. MILLER and D. F. HORNING, *J. Chem. Phys.* **34**, 265 (1961).

Table 2. Infrared spectra of mixed crystals of $H_2O_2-D_2O_2$ (frequencies in cm^{-1})

Assignments	A*	B	C	D	E	F	Assignments
ν_{OH}^\dagger	~3400 sh	3400 sh	~3400 w	~3400 w	~3395 w	~3390 vw	$\nu_{OH}(HDO)^\dagger$
ν_1	3236 s	3275 w	{~3265 sh	{~3265 sh	{3255 sh	{—	$\nu(OH \dots OH)^\ddagger$
	—	~3220 (?)	{~3215 sh	{3236 sh	{3236 vs	{3236 m	$\nu_{OH}(HDO_2)$
ν_5	3188 vs	3190 vs	{3185 vs	{~3210 vs	{3208 sh	{3208 sh	$\nu(OH \dots OH)-$
	3000 vw?	—	—	—	~3120 vw	3120 w	$\nu_{OH}(HDO)^\dagger$
$\nu_3 + \nu_6$	2847 w	2847 w	~2840 vw	~2840 vs	~2850 vs	~2850 vs	?
$2\nu_8$	2746 w	2746 w	2746 w	2754 w	2754 w	2754 w	$2\delta_{OH}(HDO_2)$
	—	—	—	~2520 vw	~2530 s	2527 s	ν_{OD}^\dagger
$\nu_{OH}(HDO)^*$	2500 vw	—	—	—	—	—	—
$\nu(OD \dots OD)^\ddagger$	—	2408 sh	{~2415 sh	2420 s	2428 s	2439 s	ν_1
$\nu_{OD}(HDO_2)$	2396 m	2386 s	{~2390 s	—	—	—	—
$\nu(OD \dots OD)-$	—	2377 sh	{~2370 sh	2376 vs	2375 vs	2375 vs	ν_5
	—	—	—	—	—	~2350 sh	ν_{OD}^\dagger
$\nu_{OH}(HDO)^*$	2300 vw	2300 vw	—	—	~2300 sh	—	—
?	~2080 vw	~2080 vw	~2080 sh	~2090 sh	~2090 sh	~2090 sh	$\nu_3 + \nu_6$
$2\delta_{OH}(HDO_2)$	~2040 vw	~2045 w	2048 w	2047 w	2044 w	2041 w	$2\nu_6$
	—	—	—	1460 sh	1460 vw	1460 vw	$\delta(HDO)$
ν_6	1409 m	1405 m	1410 sh	{~1410 sh	{~1410 sh	{1397 w	$\delta_{OH}(HDO_2)$
	1385 m	1385 m	~1390 m	{1397 m	{1397 m	{1385 sh?	$2-\nu_{OH}(HDO_2)^\ddagger$
$2\nu_4$	1330 w	1330 w	1330 w	~1385 sh	~1385 sh	—	—
	—	—	—	~1200 w	~1200 w	—	$\nu_2(D_2O)^\dagger$
	—	—	1095 vw?	1095 vw	1095 vw	~1090 vw	—
$\delta_{OD}(HDO_2)$	1049 w	1049 m	1048 m	{~1065 sh	~1065 sh	1066 sh	—
$2-\nu_{OD}(HDO_2)$	1019 vw	1019 w	1018 w	{1049 m	{1049 m	{1048 m	ν_6^\dagger
	—	—	—	{~1020 sh	{1025 sh	{1024 w	$2\nu_4$
	—	—	—	—	990 vw	991 vw	—
ν_3	881	881	881.5	882 m	882 m	882 m	ν_3
	—	—	800 sh	800 sh	800 sh	800 sh	$\nu_R(HDO)^\ddagger$
$\nu_{R_x}(H_2O_2)$	804 w	798 w	770	760 sh	760	758 vw	$\nu_R(HDO)^\ddagger$
ν_4	687 m	689 s	695 sh	{740 w	{~740 vw	{705 w	$\tau_{OH}(HDO_2)$
	—	—	681 m	{704 m	{703 w	{~685 vw	$\nu_R(HDO_2)$
$\nu_{R_x}(H_2O_2)$	648 m	654 s	~670 sh	683 w	—	—	—
$\nu_2(HDO)^\ddagger$	—	—	600 sh	600 sh	—	—	—
$\nu_2(HDO)^\ddagger$	576 vw	582 vw	585 vw	585 sh	—	—	—
	—	{565 vw	{565 w	565 sh	590 w	591 m	$\nu_{R_x}(D_2O_2)$
$\tau_{OD}(HDO_2)$	529 w	{529 m	{526 s	525 vs	523 m	514 s	ν_4
$\nu_2(HDO_2)$	~510 vw	{508 w	{507 m	506 s	505 m	—	—
	—	—	—	~495 sh	~485 sh	486 vs	$\nu_{R_x}(D_2O_2)$

* Isotopic composition of mixtures in Table 3.

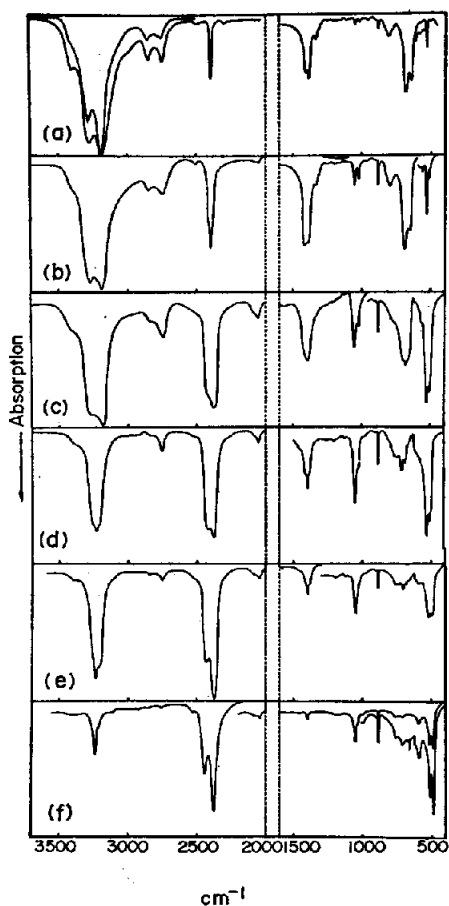
† Bands of the dihydrate.

‡ In phase—Out of phase.

subsequent authors [4, 11] in that the B_1 and B_2 classes are interchanged. The distribution of the various degrees of freedom of the Bravais unit cell, including the lattice modes, among the crystal symmetry classes is shown in Table 5. In order to describe the rotary lattice modes it is convenient to use the frame of reference of the isolated molecule in which the O—O bond defines the x -direction, and the molecular C_2 -axis the z -direction. Using this basis, the various librational modes are designated $R_{x,y,z}$ depending on the molecular axis around which the molecules are undergoing restricted rotation. The translatory vibrational modes are simply referred to as

Table 3. Approximate % composition of the isotopic mixtures

Mixtures	Bulk composition		Isotopic species		
	H_2O_2	D_2O_2	H_2O_2	HDO_2	D_2O_2
(A)	5	95	—	10	90
(B)	25	75	6	37	57
(C)	38	62	15	47	38
(D)	52	48	30	50	20
(E)	80	20	65	30	5
(F)	95	5	90	10	—

Fig. 2. Infrared spectra of isotopic mixtures of H_2O_2 and D_2O_2 having compositions shown in Table 3. Crystallization temperature about 80°K .

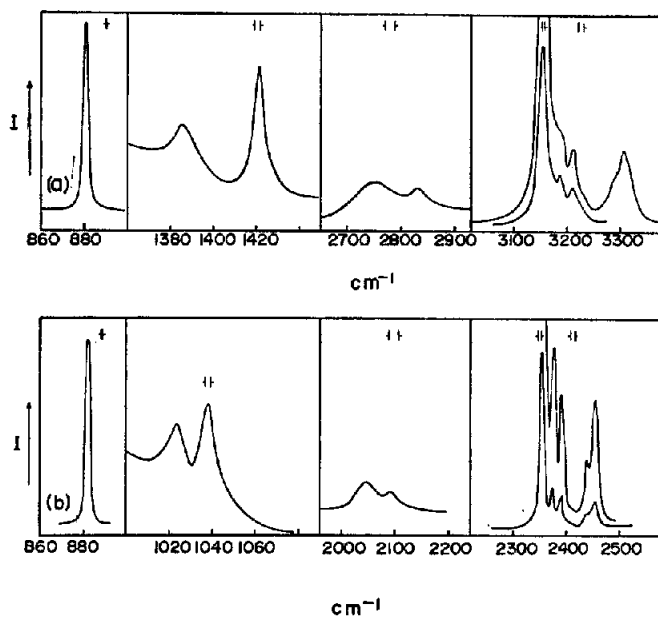


Fig. 3. Raman spectra of crystalline H_2O_2 (A) and D_2O_2 (B) in the region of the fundamental vibrations at about 80°K .

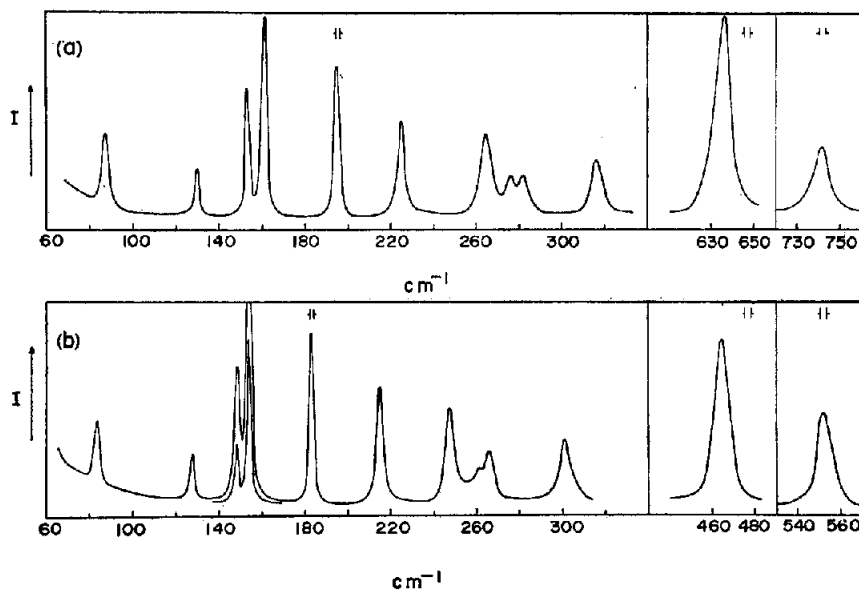


Fig. 4. Lattice vibrations of H_2O_2 (A) and D_2O_2 (B) crystals in the Raman effect at 80°K .

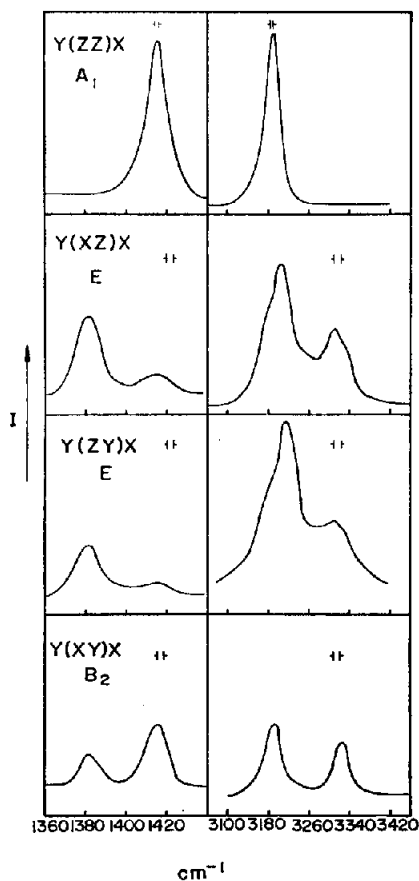


Fig. 5. Polarized Raman spectra of an oriented single crystal of H_2O_2 at 240°K .

$T(X)$, where X identifies the symmetry class. The R_g mode has been referred to as ν_7 by previous authors [4, 17].

The OH (OD) stretching vibrations

Four Raman and two i.r. bands have been reported previously for H_2O_2 in the 3μ region. The present Raman spectra show the five expected components for both H_2O_2 and D_2O_2 . In the i.r. spectra, the third predicted component could be resolved only in the case of D_2O_2 since the OH bands are nearly 50 per cent broader than are the corresponding OD bands. The effect of temperature on the OH frequencies is clearly shown in Table 1 and emphasizes some of the difficulties in correlating earlier results. The average separation of ν_1 and ν_5 (some 60 cm^{-1}) is significantly greater than in the free molecule (10 cm^{-1}) [18] because of crystal interactions.

The vibrational frequencies of the hybrid molecule, HDO_2 , can be obtained from

[18] R. L. REDINGTON, W. B. OLSON and P. C. CROSS, *J. Chem. Phys.* **36**, 1311 (1962).

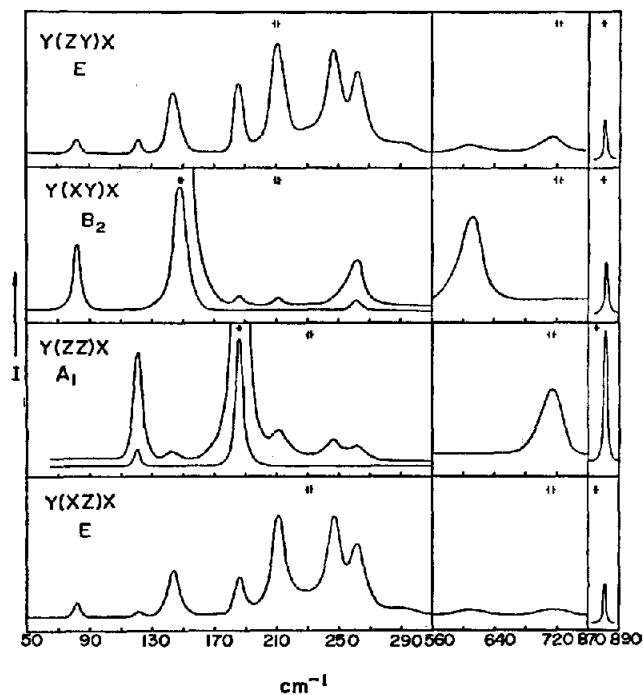


Fig. 6. Polarization characteristics of the lattice vibrations of a single crystal of H_2O_2 in the Raman effect.

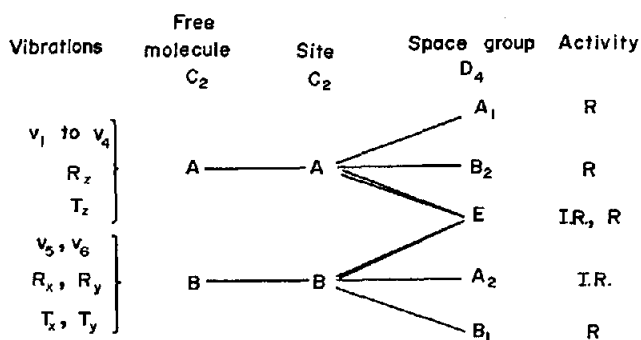


Fig. 7. Correlation diagram for the symmetry species of gaseous and crystalline H_2O_2 .

the spectra of the more dilute isotopic mixtures (Fig. 2A and 2F) in which the vibrations of the "impurity" group are not coupled dynamically with the rest of the lattice. The OD stretching frequency of HDO_2 (2396 cm^{-1}) was observed to be nearly the same as the average of the component frequencies in pure D_2O_2 , $\nu_m = 2394 \text{ cm}^{-1}$. For the OH stretching, the agreement was not as close (3236 vs. 3213 cm^{-1}). A similar situation obtains in the case of hexagonal ices where the discrepancy (in ordinary ice) is still larger: some 57 cm^{-1} .

The OH (OD) deformation vibrations

The OH and OD bending regions in the spectra could not be interpreted as satisfactorily as the stretching regions. For example, only two bands were observed in the Raman spectra instead of the expected five and their isotopic ratio (1.37) is higher than that of the stretching modes (1.34) whereas the reverse usually is true. The polarization data indicate that these bands are complex. The situation is complicated by the fact that the overtones of the internal torsion and the R_g librational modes fall in this same region and may interact with the deformations to some extent. These torsional modes also are likely to show relatively large anharmonic effects. We believe that the lower frequency band at 1332 cm^{-1} (990 cm^{-1})* in the i.r. spectrum must be a combination band. This is substantiated by the spectrum of HDO_2 which shows two well resolved bands in the OD bending region, 1048 and 1020 cm^{-1} . Clearly the latter, which is weaker, is not a fundamental. Our assignment to an overtone seems more likely than the combination ($529 + 505\text{ cm}^{-1}$) in view of the large expected anharmonicity. The corresponding band in the OH bending region is not resolved probably because the fundamental at 704 cm^{-1} is much weaker than its deuterated counterpart.

Previously, the medium intensity band at 1410 cm^{-1} in the i.r. spectrum was assigned to the symmetric bending mode [9], more precisely [17] to $\nu_2(E)$. However, in the absence of a corresponding Raman band, this must be changed to $\nu_6(A_2)$. Furthermore, from geometrical considerations, it appears that the ν_2 modes, while not forbidden in the i.r. must be exceedingly weak and may be smaller than that of ν_2 in the water molecule by almost an order of magnitude. Our assignment of the very faint band at 1065 cm^{-1} to ν_2 of D_2O_2 in the dihydrate is based on its intensity variations in different samples. Contrary to the situation in the OH stretching region, the frequencies of the OH deformation bands in the crystal do not agree too closely with those in the liquid: namely, 1400 cm^{-1} (1013 cm^{-1}) for ν_2 in the Raman effect [19] and 1350 cm^{-1} (1005 cm^{-1}) for ν_6 in the i.r. [2]. The difference seems larger than the uncertainty in location of the maxima of the broad bands in the liquids.

Interpretation of the relative intensities of the bending bands poses more problems than do the frequencies. Generally speaking the shapes and intensities of these bands are much affected by imperfect crystallization and the presence of traces of water. Certainly one very puzzling feature is the weakness of the fundamental at 1024 cm^{-1} in D_2O_2 compared with its counterpart in H_2O_2 . We see no obvious explanation for this particular isotope effect.

The O—O stretching vibration

As in previous studies, only one intense, narrow band (3 cm^{-1} width at half height) was observed for this mode. Its frequency was identical, within experimental error, in the i.r. and Raman spectra, and no indication of the three expected components was obtained. The experimental evidence clearly shows that this mode not only is unaffected by the crystal environment but that it also apparently does

* Hereafter, frequencies given in parentheses refer to the corresponding bands in the isotopic molecule.

not mix with the other internal frequencies of the molecule. The normal coordinate calculations agree well with experiment insofar as crystal effects are concerned. The computed frequencies for the crystal components fall within a 4 cm^{-1} span for H_2O_2 and a 2 cm^{-1} span for D_2O_2 . The calculations thus are consistent with the fact that the crystal components of this mode are not resolved under the present experimental conditions.

It is of interest to note that the O—O frequency shifts to *higher* frequency by 1 cm^{-1} upon deuteration. This was checked repeatedly by careful narrow-slit measurements. As expected, the calculations consistently predict this mode should shift to lower values (by from 2 to 6 cm^{-1}). Though not large, this inconsistency calls for some comment. One possible explanation is a second order isotope effect resulting in a slight shortening of the O—O bond in D_2O_2 . This could raise the O—O force constant enough to compensate for the mass effect of the deuterium. A shortening of the order of 0.005 \AA (estimated by Badger's rule) would be sufficient. The possibility that this unexpected isotope shift is due to a difference between the hydrogen and deuterium bonds in the crystal does not appear likely since the same shift has been observed recently in a Raman study of H_2O_2 and D_2O_2 vapor [20].

Torsional frequency and lattice vibrations

It has been pointed out previously [9] that the torsional vibration in the crystal and the librational lattice mode in which the molecules rotate around the O—O axis should have about the same intrinsic frequency. Since the trans potential barrier in the free molecule is only about one kcal/mole [18], the main restoring force in both crystal modes comes from the hydrogen bonds. From the point of view of lattice dynamics the ν_4 and R_x modes may be thought of as symmetric and antisymmetric modes involving restricted rotation of coupled OH groups. Despite this conceptual simplification, it was found difficult to work out an acceptable assignment for the bands in the $600\text{--}820\text{ cm}^{-1}$ ($450\text{--}600\text{ cm}^{-1}$) region of the spectrum. In particular, the i.r. band at 809 cm^{-1} is puzzling. Its frequency is higher than expected for a component of either ν_4 or R_x . Indeed, the normal coordinate calculations invariably yield appreciably lower frequencies for all components of these frequencies. MILLER and HORNIG [17] assigned this band to a combination ($151 + 566 = 807$) which is reasonable since it has the correct symmetry for i.r. activity. On the other hand, the three bands at 809 , 690 and 656 cm^{-1} in the H_2O_2 spectrum have strikingly similar counterparts at 585 , 511 and 482 cm^{-1} in the D_2O_2 spectrum, none of which can be assigned as combinations. Moreover, the isotopic frequency ratios for corresponding bands fall in the range $1.30\text{--}1.36$, values which are normal for hydrogen motions and which rule out combinations with lattice modes involving significant motions of the oxygen atoms.

The symmetry assignments for the lower frequency lattice modes were fairly straightforward with only a couple of unsatisfactory aspects. One involved the doublet at $276/281\text{ cm}^{-1}$ ($260/264\text{ cm}^{-1}$). According to our polarization data, one of the components should belong to the E class. However, the i.r. spectra of H_2O_2 show no measurable absorption near 280 cm^{-1} . Tentatively, we assign the extra E

[20] P. A. GIGUÈRE and T. K. K. SRINIVASAN, Unpublished results.

symmetry band to the overtone of the strong translation band at 152 cm⁻¹ (148 cm⁻¹) Also, librational (rotatory) modes usually are relatively intense in the Raman effect while translatory modes tend to be weak. On the basis of this criterion, the strong Raman band at 161 cm⁻¹ (154 cm⁻¹) should be assigned to a rotatory mode despite its relatively low frequency. Actually, the normal coordinate calculations show that this mode, as well as most of the others, is mixed so that no simple description applies.

The hydrogen bonds

In view of the many similarities between hydrogen peroxide and water, it is logical to compare the two compounds in terms of their hydrogen bonding, the main packing force in both crystals. Various indices suggest that the hydrogen bonds in peroxide are slightly weaker than in ice. First is the appreciably longer O—H . . . O distance, 2.80 Å [13, 14] compared with 2.76 Å [21]. According to the usual empirical correlations [22] this corresponds to a decrease of some 12–15 per cent in hydrogen bond strength. Comparable values are arrived at from the decrease in the O—H stretching frequency when hydrogen bonds are formed, namely, (3610–3210) = 400 cm⁻¹ from the average of the present data, and (3705–3275) = 430 cm⁻¹ for water. A similar conclusion is reached from the temperature effect on the libration and translation lattice frequencies in the crystals which involve directly bending and stretching of the hydrogen bonds. Data for the coefficient ($\Delta\nu/\nu$) per °C for ordinary ice [23] and for peroxide from the present as well as previous work [9] follow:

$$\begin{aligned} \nu_R(\text{H}_2\text{O}_2) &= -2.6 & \nu_T(\text{H}_2\text{O}_2) &= -3.5 \\ \nu_{R_2}(\text{H}_2\text{O}_2) &= -2.4 & \nu_{T'}(\text{H}_2\text{O}_2) &= -3.2 \end{aligned}$$

This slightly lower hydrogen bond energy in the peroxide crystal may be due to a lesser polarity of the O—H bond and/or the less symmetrical balance of forces about each molecule because of the two unengaged lone-pair orbitals of the oxygen atoms.

It is interesting to note that the O—H stretching bands are much narrower in the peroxide crystal than in ice [24], (Table 4). The unusual width in the case of water is due in part to Fermi resonance with the overtones of bending modes which does not occur in hydrogen peroxide. Furthermore, the peroxide crystal is ordered in contrast to ice where the disorder of the protons must contribute to the abnormal width of the O—H bands. Another remarkable feature of these bands is their greatly reduced width in the Raman spectrum (Fig. 3) compared with the i.r. Although the Raman spectra were obtained from single crystals while the i.r. samples were microcrystalline, it does not appear *a priori* that crystal imperfections and reflection losses can account for the observed differences. The often invoked combinations with low-frequency lattice modes do not apply here for several reasons:

- [21] S. PETERSON and H. LEVY, *Acta Cryst.* **10**, 70 (1957).
 [22] G. C. PIMENTEL and A. L. McCLELLAN, *The Hydrogen Bond*. W. H. Freeman, San Francisco (1960).
 [23] R. ZIMMERMANN and G. C. PIMENTEL, *Advances in Molecular Spectroscopy*, p. 726. Pergamon Press, (1962).
 [24] D. EISENBERG and W. KAUZMANN, *The Structure and Properties of Water*, p. 128. Clarendon Press, Oxford, (1969).

Table 4. Approximate half-widths (in cm^{-1}) of the O—H and O—D stretching bands in various crystals

	Raman	I.R.		Raman	i.r.
H_2O_2	20	80	H_2O	~40	~500
D_2O_2	12	50	D_2O	~25	~300
$\text{HDO}_2(\text{OH})$	11	22	$\text{HDO}(\text{O—H})$	—	~50
$\text{HDO}_2(\text{O—D})$	8	15	$\text{HDO}(\text{O—D})$	—	~30

Table 5. Distribution of the degrees of freedom of crystalline hydrogen peroxide among symmetry classes

Symmetry class	Total Deg. of F.	Unit cell translations	Translatory modes	Librational modes	Internal modes
A_1	6	0	1	1	4
A_2	6	1	1	2	2
B_1	6	0	2	2	2
B_2	6	0	1	1	4
E	12	1	2	3	6

(a) the number of possibilities is rather limited (b) such combinations should also appear in the Raman effect, and (c) the half-widths of the O—H bands show a constant ratio of $\sqrt{2}$ to those of the O—D. It also is noteworthy that a drop of some 160° in the temperature of the peroxide crystal reduces in half the width of all the OH bands in the Raman spectrum, whether of molecular or lattice origin. (Compare Fig. 3 and 4 with Fig. 5 and 6). In contrast the O—O stretching band remains unaltered because it is not directly affected by hydrogen bonding.

NORMAL COORDINATE CALCULATIONS

A characteristic feature of the hydrogen peroxide crystal is the relatively strong and directed intermolecular forces resulting from the hydrogen bonds present. In as much as these hydrogen bonds effectively act as very weak chemical bonds in the crystal, they must be taken into account explicitly by any normal coordinate treatment of the crystal spectrum. For purposes of the analysis, a "molecule unit" was defined which is shown schematically in Fig. 8. In addition to a central H_2O_2 molecule, this unit includes two H atoms and two O atoms from neighboring molecules linked to the central H_2O_2 molecule by hydrogen bonds. A similar type of model has been used in the analysis of the vibrational spectrum of liquid water [25] and ice [26]. This unit served to define a basis set of internal coordinates in terms of which the normal coordinate analysis was carried out. In addition to internuclear distances representing the normal chemical bonds, the H . . . O hydrogen bonds, the molecular valence angles and the angles involving the hydrogen bonds, two additional distances were included in the basis set. These were the two close H . . . H distances since it was felt there would be sufficient interaction to warrant their

[25] R. A. M. O'FERRAL, G. W. KOEPL and A. J. KRBSGE, *J. Am. Chem. Soc.* **93**, 1 (1971).

[26] Y. KYOGOKU, *J. Chem. Soc. Jap., Pure Chem. Sec.* **81**, 1648 (1960).

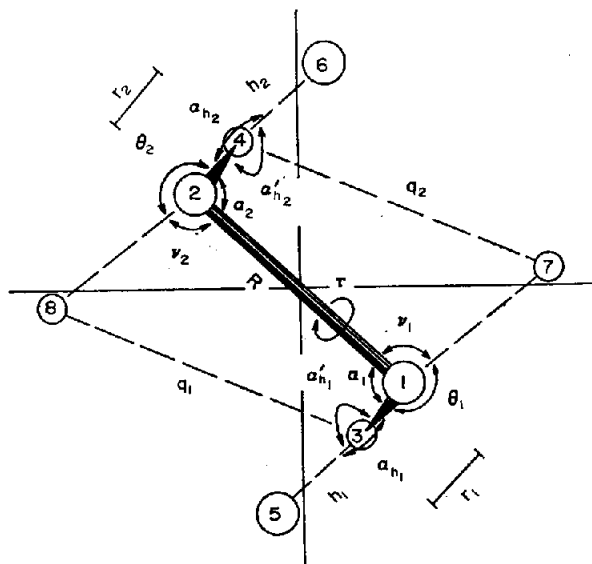


Fig. 8. Model showing internal coordinates used in the vibrational analysis of the spectrum of crystalline hydrogen peroxide. (The angle, α_h , refers to the in-plane bending, and the angle, α'_h , to the out-of-plane bending of the OH groups.)

inclusion. Although the neutron diffraction results [14] show that the proton in the O—H . . . O linkage does not quite lie on the line between the two oxygen atoms, the deviation is small and the hydrogen bonds were assumed linear in the model.

Using the coordinates depicted in Fig. 8, the set of symmetry coordinates shown in Table 6 was obtained on the basis of the local C_2 symmetry of the unit. These

Table 6. Symmetry coordinates for extended H_2O_2 molecule having local C_2 symmetry

Coordinate	Description
A Class	
$S_1 = a(\Delta r_1 + \Delta r_2)$	OH symmetric stretch
$S_2 = a(\Delta \alpha_1 + \Delta \alpha_2)$	OOH symmetric deformation
$S_3 = \Delta R$	O—O stretch
$S_4 = \Delta R$	O—O torsion
$S_5 = a(\Delta h_1 + \Delta h_2)$	OH . . . O symmetric stretch
$S_6 = a(\Delta \alpha_{h1} + \Delta \alpha_{h2})$	OH . . . O symmetric linear bending
$S_7 = a(\Delta \alpha'_{h1} + \Delta \alpha'_{h2})$	OH . . . O symmetric linear bending
$S_8 = a(\Delta \theta_1 + \Delta \theta_2)$	H . . . OH symmetric deformation
$S_9 = a(\Delta \gamma_1 + \Delta \gamma_2)$	H . . . OO symmetric deformation
$S_{10} = a(\Delta q_1 + \Delta q_2)$	H . . . H stretch
B Class	
$S_{11} = a(\Delta r_1 - \Delta r_2)$	OH asymmetric stretch
$S_{12} = a(\Delta \alpha_1 - \Delta \alpha_2)$	OOH asymmetric deformation
$S_{13} = a(\Delta h_1 - \Delta h_2)$	OH . . . O asymmetric stretch
$S_{14} = a(\Delta \alpha_{h1} - \Delta \alpha_{h2})$	OH . . . O asymmetric linear bending
$S_{15} = a(\Delta \alpha'_{h1} - \Delta \alpha'_{h2})$	OH . . . O asymmetric linear bending
$S_{16} = a(\Delta \theta_1 - \Delta \theta_2)$	H . . . OH asymmetric deformation
$S_{17} = a(\Delta \gamma_1 - \Delta \gamma_2)$	H . . . OO asymmetric deformation
$S_{18} = a(\Delta q_1 - \Delta q_2)$	H . . . H stretch
$a = 1/\sqrt{2}$	

local symmetry coordinates were then used to construct symmetry coordinates for the five symmetry classes of the optically active vibrational modes of the crystal. Elements of the inverse kinetic energy (G) matrix for the molecule unit were obtained by standard methods [15, 27] and transformed into the symmetry coordinate basis. Molecular dimensions were taken from the neutron diffraction results [14] with the approximation noted above. Adjustment of trial valence symmetry force constants was carried out on an IBM 360/67 computer using a standard iterative least squares program similar to those described elsewhere [28-31]. In several of the symmetry classes, assignments for specific frequencies were missing or uncertain due to possible accidental degeneracies. In these cases, zero or small weights were attached to estimated experimental values to remove them from the refinement process.

Observed and calculated frequencies for the five symmetry classes of the factor group of the unit cell are listed in Table 7 together with the potential energy distributions expressed in terms of the local symmetry coordinates listed in Table 6. The potential energy terms are given as percentages with only the principal contributions included. The potential energy distributions for D_2O_2 are not tabulated since, with only a very few exceptions, the distributions within the individual modes were quite similar to those of the corresponding hydrogen modes. In the computations, the frequencies of the normal and deuterated species were fitted simultaneously to the same set of force constants with the exception of the OH and OD stretching modes. Since the latter frequencies are well removed from the rest of the spectral bands, and since anharmonicity effects are most pronounced in these modes, separate values of the O—H force constant were used to fit the OH and OD stretching frequencies. As a consequence, these high frequencies could be fitted with somewhat reduced discrepancies between observed and calculated values which in turn aided in fitting the lower frequencies. In general, the agreement between the observed and calculated values for the 59 assigned frequencies of the two isotopic species was satisfactory and within the limitations imposed by the model and the neglect of anharmonicity. A few aspects of the calculated spectrum, however, deserve comment. The two molecular modes, ν_1 and ν_5 , each split into three components (Fig. 7) as a result of interactions among the molecules in the unit cell. In the case of ν_1 , the assignments place the B_2 and E components relatively close together at 3304 and 3285 cm^{-1} but well separated from the A_1 component which is observed at 3155 cm^{-1} . The calculated values on the other hand show the components to be uniformly spaced about 55 cm^{-1} apart. The B_1 and E components of ν_5 likewise occur fairly close together at 3208 and 3187 cm^{-1} and again the calculated components are uniformly spaced with about the same separation as for the calculated ν_1 components. This difference between the observed and calculated splitting patterns for the two fundamentals may arise as a result of a Fermi type interaction between the two E components of

[27] T. SHIMANOUCI, M. TSUBOI and T. MIYAZAWA, *J. Chem. Phys.* **35**, 1597 (1961).

[28] J. OVEREND and J. R. SOHRERER, *J. Chem. Phys.* **32**, 1289 (1960).

[29] J. ALDOUS and I. M. MILLS, *Spectrochim. Acta* **18**, 1073 (1962).

[30] T. SHIMANOUCI, *Computer Programs for Normal Coordinate Treatment of Polyatomic Molecules*. Dept. of Chemistry, Faculty of Science, University of Tokyo, July (1968).

[31] R. C. TAYLOR, H. S. GABELNICK, K. AIDA and R. L. AMSTER, *Inorg. Chem.* **8**, 605 (1969).

Table 7. Observed and calculated frequencies and potential energy distribution for crystalline hydrogen and deuterium peroxide

Observed	H_2O_2 Calc.	Δ	Potential energy distribution for H_2O_2	Observed	D_2O_2 Calc.	Δ
<i>A₁</i> Class						
3155	3188	-33	96- S_1 , 4- S_8	2353	2369	-16
1421	1429	-8	74- S_2 , 19- S_9 , 5- S_6	1038	1046	-8
881	885	-4	79- S_3 , 9- S_9 , 8- S_2	882	879	3
742	742	0	44- S_9 , 30- S_7 , 13- S_8	553	570	-17
195	198	-3	63- S_8 , 19- S_7 , 9- S_9	184	184	0
131	135	-4	51- S_5 , 25- S_7 , 15- S_8	127	127	0
<i>A₂</i> Class						
—	3124	—	95- S_{11} , 5- S_{13}	—	2336	—
1410	1430	-20	72- S_{12} , 16- S_{16} , 5- S_{14}	1048	1057	-9
656	681	-25	34- S_{16} , 34- S_{17} , 24- S_{16}	486	495	-9
236	240	-4	53- S_{16} , 23- S_{13} , 9- S_{14}	230	235	-5
109	100	9	36- S_{13} , 22- S_{14} , 20- S_{15}	105	95	10
<i>B₁</i> Class						
3208	3239	-31	95- S_{11} , 4- S_{13}	2391	2408	-17
1385	1377	8	88- S_{12} , 7- S_{14}	1023	1020	3
423	447	-24	46- S_{17} , 35- S_{15} , 17- S_{16}	357	341	16
280	281	1	78- S_{13} , 8- S_{11} , 5- S_{18}	274	272	2
—	79	—	65- S_{15} , 25- S_{16}	—	74	—
—	66	—	50- S_{16} , 38- S_{15} , 6- S_{17}	—	64	—
<i>B₂</i> Class						
3304	3300	4	96- S_1 , 3- S_6	2434	2441	-7
1385	1407	-22	88- S_2 , 6- S_8	1023	1036	-13
881	883	-2	83- S_3 , 9- S_2 , 5- S_9	882	881	1
637	627	10	56- S_9 , 19- S_7 , 8- S_8	467	519	-52
161	164	-3	37- S_7 , 31- S_6 , 11- S_{10}	164	162	2
87	—	—	—	84	—	—
<i>E</i> Class						
3285	3245	40	96- S_1 , 3- S_6	2440	2405	35
3187	3181	6	95- S_{11} , 5- S_{13}	2376	2371	5
1421	1418	3	78- S_2 , 5- S_9 , 5- S_{12}	1038	1039	-1
1385	1371	14	76- S_{12} , 5- S_{14} , 6- S_2	1023	1014	9
881	883	-2	82- S_3 , 8- S_2 , 5- S_9	882	880	2
690	678	12	34- S_9 , 20- S_{15} , 14- S_{16}	591	530	61
—	602	—	30- S_{17} , 29- S_7 , 13- S_8	514	455	59
264	276	-12	51- S_{15} , 17- S_{13} , 14- S_{16}	248	236	12
225	221	4	47- S_6 , 21- S_{12} , 16- S_8	216	216	0
152	151	1	60- S_{16} , 21- S_{15} , 5- S_{17}	149	145	4
109	74	35	58- S_8 , 16- S_7 , 14- S_{16}	105	71	43

the two fundamentals which perturbs their positions. The situation is essentially the same for the OD bands.

In the OOH (OOD) deformation region, the splitting pattern for the ν_2 components again is predicted by the calculations to be an evenly spaced triplet; however, in the case of ν_6 , the B_1 and E components are calculated to be nearly degenerate and separated significantly from the A_2 component. Unfortunately, only two bands could be distinguished in the Raman spectrum and experimental corroboration is consequently inconclusive.

Among the remaining frequencies, the most marked discrepancies between observed and calculated values occur in the three deuterium peroxide bands discussed

earlier at 467, 514 and 591 cm^{-1} and assigned respectively to B_2 , E and E modes. These three bands deviate from the calculated values by amounts appreciably greater than the average deviation of the remaining frequencies. It is worthy of note that the isotopic frequency ratios of the calculated frequencies of these three bands range from 1.21 to 1.32, values which are significantly lower than the ratios of experimental frequencies if the 809 cm^{-1} band of H_2O_2 is taken as a lattice fundamental. Since polarization measurements were not done on the D_2O_2 crystal, evidence for symmetry assignments depends chiefly on whether a given band appeared in the Raman or i.r. spectrum, or both. Such evidence provided the basis for assigning the 467 cm^{-1} band as a B_2 mode and the 514 cm^{-1} band as an E mode, although the calculated frequencies would agree better with the reverse assignment.

Individual valence force constants defined in terms of the coordinates shown in Fig. 8 are listed in Table 8. In all, eleven principal constants and twenty interaction constants were used to reproduce the calculated values shown in Table 7. A number of the possible interaction constants were eliminated at the start of the calculations on the basis that they linked non-adjacent coordinates (coordinates having no common atom) and therefore were likely to be quite small and non-determinable with the available data. Such constants, for example, include interactions between internal coordinates belonging to two different molecules in the unit cell. The sensitivity of the calculated frequencies to the remaining interaction constants was explored by trial and error and those constants which had no significant effect on the frequencies, or which had large dispersions, were also constrained to zero. The final potential function represented by the constants in Table 8 therefore constitutes a satisfactory although not necessarily unique solution to the vibrational problem of the crystal. The only previous analysis of the crystal spectrum is that of MILLER and HORNIG [17]. They did not attempt to deal with any of the lattice modes occurring below 600 cm^{-1} and included only the R_g librational lattice mode explicitly.

The force constants of the peroxide unit cell can be divided into two groups, one consisting of the intramolecular constants and the other the lattice constants. Comparison of the results with those for the ice system based on a comparable model [26] is complicated by the fact that the investigator used a Urey-Bradley type of potential function. However, the O—H stretching constant from the present work is slightly less than the value reported by KYOGOKU [26] for ice which is in accord with the data which suggest that the OH bond in ice is slightly stronger than in peroxide. The value reported by MILLER and HORNIG is appreciably larger than that found here but any comparison does not appear significant in view of the difference in assignments. The remaining three principal intramolecular force constants are about of the magnitude to be expected, the O—O constant in particular agreeing very closely with the value predicted by Badger's rule. The small value found for the torsion constant, 0.042 $\text{md}/\text{\AA}$, lends support to the prediction that the restoring forces controlling the librational motions of the OH groups in the crystal arise chiefly from the intermolecular hydrogen bonds. The very small value of this constant also undoubtedly is responsible for the fact that no torsional mode is identified by the potential energy distributions, although a contributing factor also is the fact that the two coordinates, S_4 and S_9 , are not completely independent.

Table 8. Force constants and dispersions for hydrogen peroxide in the crystalline state

Force constant	δ	Force constant	δ		
$f_r(\text{OH})$	5.529	0.040	$f_{r,h}$	0.116	0.020
$f_{r\text{OD}}$	5.815	0.056	$f_{a,\theta}$	0.026	0.009
f_a	0.950	0.023	$f_{r',h}$	-0.033	0.013
f_R	3.999	0.031	$f_{r,ah}$	-0.032	0.016
f_r	0.042	0.023	$f_{r,\theta}$	-0.031	0.015
f_h	0.255	0.011	$f_{h,h}$	-0.028	0.010
f_{ah}	0.032	0.011	$f_{h,ah'}$	-0.012	0.004
f_θ	0.157	0.006	f_{ah,θ^*}	-0.049	0.006
f_γ	0.588	0.025	f_{ah',θ^*}	-0.094	0.003
f_{ah}	0.074	0.004	f_{ah,γ^*}	-0.020	
f_a	0.033	0.009	f_{ah',γ^*}	-0.076	0.004
			f_{θ,θ^*}	0.065	0.008
			f_{θ,γ^*}	0.090	
			f_{a,θ^*}	-0.006	0.010
$f_{r,r}$	0.140	0.040			
$f_{a,a}$	0.027	0.023			
$f_{r,R}$	0.447	0.961			
$f_{R,a}$	0.679	0.106			
$f_{r,a}$	0.426	0.121			

Units: stretch, mdyne/Ang.; stretch-bend, mdyne; bend, mdyne-Ang.

* Coordinates involved belong to two different molecule units.

The only other intramolecular constant about which a comment could be made is f_{rr} , the OH—OH interaction constant. In the free molecule, this constant has a negative sign [32] whereas in the crystal, it is positive. Since this constant is determined by the separation between the ν_1 and ν_6 fundamentals, the change in sign emphasizes the fact that the relative positions of these two modes are interchanged on going from the gas to the crystal.

Of the lattice constants, the one of most interest is f_h , the force constant of the hydrogen bond. The value found here for crystalline H_2O_2 is $f_h = 0.255 \text{ md/\AA}$ which can be compared with the value of 0.19 md/\AA for ice [26] and the value of 0.12 md/\AA for water [25]. However, any discussion based on numerical comparisons does not appear profitable because of differences in potential functions. In particular, the present potential function includes an interaction constant between the O—H stretch and the hydrogen bond stretch, $f_{r,h}$, which other investigators did not include. The addition of this interaction constant significantly improved the fit in the present calculations but the hydrogen bond constant, f_h , increased in magnitude as a result. Valid arguments have been cited previously for believing that the hydrogen bond in hydrogen peroxide is somewhat weaker than that in water or ice. One is therefore left with the conclusion that the $f_{r,h}$ interaction constant probably is a significant one which should be included explicitly in any potential function involving hydrogen bonds. Discussion of the values obtained for the other lattice constants does not appear to be particularly fruitful. Most of the numbers obtained appear to be of the expected numerical magnitude and are comparable with values in the literature.

[32] E. HIROTA, *J. Chem. Phys.* **28**, 839 (1958).

The constant associated with the non-bonded H . . . H distance was quite small and did not contribute significantly to fitting the observed frequencies.

In conclusion, one can note that thirty one force constants have been used in the present treatment to reproduce some fifty nine assigned frequencies for crystalline H_2O_2 and D_2O_2 . The agreement between observed and calculated frequencies is quite satisfactory and the values obtained for the intramolecular and lattice force constants are reasonable and compare in magnitude to those obtained in other hydrogen bonded systems. The model on which the calculations are based, although simplified, is realistic and has provided a satisfactory interpretation of the vibrational spectra. Although some uncertainties still exist regarding the identification and assignment of certain of the crystal frequencies, it does not appear that their clarification will affect the results in any major way.

Acknowledgement—The authors are indebted to Dr. S. TREVINO for his interest and for communications regarding the ambiguity in the identification of the B_1 and B_2 symmetry classes. The Canadian authors are grateful to the National Research Council of Canada for a continuing research grant.